

Thesis for the degree of Doctor of Philosophy

Rheological Response to Tectonic and Volcanic Deformation in Iceland

Md. Tariqul Islam



UNIVERSITY OF GOTHENBURG

FACULTY OF SCIENCE

Doctor Thesis A160
University of Gothenburg
Department of Earth Sciences
Gothenburg, Sweden 2016

ISBN 978-91-628-9796-3 (PDF)
ISBN 978-91-628-9797-0 (Print)

Md. Tariqul Islam

Md. Tariqul Islam

Rheological response to tectonic and volcanic deformation in Iceland

A160-2016

ISBN 978-91-628-9796-3 (PDF)

ISBN 978-91-628-9797-0 (Print)

ISSN 1400-3813

Internet ID: <http://hdl.handle.net/2077/42079>

Printed by Ineko AB

Copyright © Md. Tariqul Islam 2016

Distribution: Department of Earth Sciences, University of Gothenburg, Sweden

Abstract

Iceland is one of the few places in the world where a Mid-Oceanic Ridge (MOR) is exposed on land, and this gives good opportunity to study geodynamic processes. Spreading of Mid-Atlantic Ocean Ridge (MAR) segments in Iceland began ~60 million years ago. The MAR segments in Iceland have a divergent spreading rate between the Eurasian and North American plates of ~19 mm yr⁻¹ and are divided into the Western (WVZ), Eastern (EVZ), and Northern Volcanic Zones (NVZ). These zones include 35 active volcanic systems and most of them are located on the plate boundaries. Often a volcanic system consists of a central volcano and an associated fissure swarm. Geothermal activities and Glacial Isostatic Adjustment (GIA) in Iceland occur in addition to the tectono-volcanic activities, adding to the complexity of the geodynamic investigation.

Crustal deformations due to tectonic and volcanic activities in Iceland have been studied with geodetic observations since 1938. This study uses geodetic Global Positioning System (GPS) data (1994–2015) collected in the WVZ, EVZ, and NVZ. These measurements suggest that the spreading velocities along profiles parallel to spreading directions are 6.7 ± 0.5 mm yr⁻¹ (crossing Thingvellir graben) in the WVZ, 14.0 ± 2 mm yr⁻¹ (between south of Vatnajökull glacier and Torfajökull volcanic system) in the EVZ, and 18.4 ± 1.5 mm yr⁻¹ (crossing Fremri Námur volcanic system) in the NVZ. The widths of the deformation zones along those profiles are ~50 km in the WVZ, ~100 km in the EVZ, and ~56 km in the NVZ, where ~85–90% of the deformations are accumulated. At the center of Thingvellir rift graben in the WVZ, continuous subsidence of ~4 mm yr⁻¹ is observed, whereas uplift is dominant in the NVZ and the EVZ. After GIA corrections, the western and eastern parts of the EVZ are dominated by uplifting and subsidence, respectively. In the NVZ, subsidence caused by plate stretching is mostly compensated by magmatic activities in the form of dyke intrusion. However, the center of the rift and the maximum subsidence geographically coincides in the WVZ and the NVZ, whereas in the EVZ, the maximum subsidence is offset ~8 km to the east of the spreading center. In the NVZ, the Askja volcano has a stretched magma chamber at a shallow depth (~3.5 km). GPS observations made between 2008 and 2013 at the Askja volcanic system suggests that absolute subsidence in the center of this volcanic system is 11.9 ± 0.1 mm yr⁻¹ in International Terrestrial Reference Frame 2008. After GIA correction, this subsidence rate is ~30 mm yr⁻¹ and the subsidence is caused by activities in the magma chamber. However, subsidence in Askja is decaying exponentially with time. On the other hand, in the isolated volcanic system of Surtsey, which is free of tectonic and GIA activities, GPS and leveling observations between 1992 and 2013 suggest that average subsidence rate is decaying: ~10 mm yr⁻¹ between 1992 and 2000, ~8 mm yr⁻¹ between 2000 and 2002, and ~3 mm yr⁻¹ between 2002 and 2013. This subsidence is caused by the compaction of the volcanogenic material and lithostatic loading of the erupted material. However, today there is very little vertical deformation. This study uses temperature dependent rheological Finite Element (FE) modeling to analyze the crustal deformations of plate spreading and volcano-tectonic activities. Thermal properties in the models are taken from earlier thermal studies in Iceland. The models also account for dislocation, diffusion, and composite (the combined effect of dislocation and diffusion) in both wet and dry conditions. The 700°C isotherm is applied for long term brittle-ductile transition.

Rheological responses differ in horizontal and vertical directions. The thermal state has the greatest influence in deformation process with steady state velocity. Wet and dry rheological models give more or less similar results; however, dry rheological models provide slightly better results. In the rift zone of divergent rift environment in Iceland, the dominant deformation is governed by dislocation creep. The depth of the 700°C isotherm at the rift axis

is 8, 13, and 6 km in the WVZ, EVZ, and NVZ, respectively. Different depths of the isotherm are governed by the configuration of volcanic systems and existence of geothermal activities

The rift zones in the WVZ and NVZ are fairly similar. In the WVZ, an overlap of two volcanic systems exists, but in the EVZ most recent activities have taken place away from the maximum subsidence of plate boundary. In the NVZ, all the spreading affects only one volcanic system (with little overlap of the neighboring systems). While in the EVZ, the geometry of the volcanic systems is very different, and five volcanic systems are arranged parallel to each other and no central volcano exists within any of these volcanic systems.

To explain the observed style of surface deformation in the EVZ, a maximum magmatic influx of $\sim 11 \text{ mm yr}^{-1}$ at 100-km depth is required to shift $\sim 10\text{--}20 \text{ km}$ west from the center of the horizontal deformations. On the other hand, the best fit model results in $\sim 4 \text{ mm yr}^{-1}$ and $\sim 15 \text{ mm yr}^{-1}$ subsidence, rates that are higher than observations due to magmatic and magmatic-tectonic activities at Askja, respectively. However, a uniform viscosity of $3 \times 10^{18} \text{ Pa s}$ for the asthenosphere and a 50-km thick lithospheric model results in 27.5 cm subsidence as the result of the load of eruptive materials in Surtsey.

Key words: Iceland, Tectono-volcanic deformation, Lithostatic loading, Geodynamic finite element model, Temperature- and stress-dependent rheology, Wet and dry rheology, Dislocation and diffusion creep.

Preface

This doctoral thesis is based on summary of following six papers. These papers are reprinted with the permission of the respective journals.

1. **Islam, M.T.**, & Sturkell, E. (submitted). Rheological responses on plate boundary deformations at the Eastern Volcanic Zone in Iceland, in *Tectonophys.*, TECTO10937.
2. **Islam, M.T.**, & Sturkell, E. (2015). Temperature-Dependent Newtonian Rheology in Advection-Convection Geodynamical Model for Plate Spreading in Eastern Volcanic Zone, Iceland, *J. Geosci. Envi. Prot.*, **3**, 14-26, doi:10.4236/gep.2015.35003.
3. **Islam, M.T.**, Sturkell, E., LaFemina, P., Geirsson, H., Sigmundsson, F., Olafsson, H. (2016). Continuous subsidence in the Thingvellir rift graben, Iceland: Geodetic observations since 1967 compared to rheological models of plate spreading, *J. Geophys. Res. Solid Earth*, **121**, 321-338, doi:10.1002/2015JB012306.
4. **Islam, M.T.**, Sturkell, E., Sigmundsson, F., LaFemina, P., Geirsson, H., & Vincent, D. (manuscript), Temperature-dependent non-linear rheological models of plate spreading in Iceland, for *Geophys. J. Int.*
5. Sturkell, E., Einarsson, E., Geirsson, H., Hjartardóttir², Á.R., **Islam, M.T.**, Moore, G.J., & Sigmundsson, F. (manuscript). Continuing subsidence and deformation of the Surtsey volcano, 1991 - 2013, Iceland, for *J. Volcanol. Geotherm. Res.*

Manuscript in progress not included in the thesis

Islam, M.T., Sturkell, F., & Vincent, D. (manuscript in progress). Volcano-tectonic interplay at the Askja volcanic system, Iceland: Finite element modeling constrained by geodetic measurements, for *J. Volcanol. Geotherm. Res.*

Table of Contents	6
Abstract	3
Preface	5
1. Introduction	11
<i>1.1. Research aims</i>	11
<i>1.2. Study area: geology and tectonic settings</i>	13
2. Surface deformations observations	16
<i>2.1. Leveling data</i>	17
<i>2.2. GPS data</i>	17
3. Modeling	18
<i>3.1 Rheology in modeling</i>	19
4. Results and Discussion	21
5. Conclusion	25
Future work	25
Acknowledgements	26
References	27
Appendix	32

List of Symbols and acronyms

Symbol	Unit	Description
MOR	-	Mid Ocean Ridge
MAR	-	Mid-Atlantic Ocean Ridge
NORDVULK	-	Nordic Volcanological Center
EVZ	-	Eastern Volcanic Zone
NVZ	-	Northern Volcanic Zone
WVZ	-	Western Volcanic Zone
HB	-	Hreppar Block
SISZ	-	South Icelandic Seismic Zone
TFZ	-	Tjörnes Fracture Zone
DZ	km	Deformation zone
GIA	-	Glacial Isostatic Adjustment
EDM	m	Electronic Distance Measurement
GPS	m	Global Positioning System
InSAR	-	Interferometric Synthetic Aperture Radar
ITRF	-	International Terrestrial Reference Frame
MORVEL	mm yr ⁻¹	Mid-Ocean Ridge VELOCITY
NUVEL	mm yr ⁻¹	A global plate motion
REVEL	mm yr ⁻¹	REcent plate VELOCities
FE/FEM	-	Finite Element Model
BC	-	Boundary Conditions
E	Pa	Young's modulus
ν	-	Poisson's ratio
A	MPa ⁻ⁿ s ⁻¹	Pre-exponential factor
σ	MPa	Differential stress
n	-	Exponent of differential stress
C_{HO}	H/10 ⁶ Si	Water content
r	-	Exponent of water content
d	μm	Grain size
i	-	Exponent of grain size
E_a/Q	kJ mol ⁻¹	Activation energy
V	10 ⁻⁶ m ³ mol ⁻¹	Activation volume
P	GPa	Pressure
ρ	kg m ⁻³	Density
m	-	Strain hardening
R	J mol ⁻¹ K ⁻¹	Universal gas constant
T	K, °C	Temperature
T_m	°C	Mantle temperature
T_s	°C	Surface temperature
C_p/C	J kg ⁻¹ K ⁻¹	Specific heat
k	mm ² s ⁻¹	Thermal diffusivity
t_r	Myr	Age of surface rock
η	Pa s	Viscosity
η_o	Pa s	Reference viscosity
η_{eff}	Pa s	Effective viscosity

To my family

Part I

Synthesis

1. Introduction

The 2% of the Mid Oceanic Ridges (MOR) exposed on land provide a natural laboratory to study the exchange of mass between Earth's interior and its solid crust and/or lithosphere, the so called geodynamic systems (Toomey 2012; Wright *et al.* 2012). About 80% of magmatic activities on Earth occur where tectonic plates separate and extruded magma cools to form new crust (Toomey 2012). Along the Mid-Atlantic Ridge (MAR), the divergent plate boundaries of the North American and Eurasian plates can be largely demarcated by mapping epicentres of earthquakes (Fig. 1). Iceland is a small segment of the MAR (Fig. 1), representing more than 41% out of the 2% that is globally exposed above sea level. Iceland, 300×500 km, is a hotspot believed to be feed by a deep mantle plume (Einarsson 2001). The MAR segment in North Atlantic (Iceland) is characterised as slow spreading (Dick *et al.* 2003). The far field stretching causes the plates to move steadily apart by ~ 19 mm yr⁻¹.

In Iceland, far field stretching is constant, but rifting at the plate boundary is episodic; spreading rate and spatial distribution along the spreading direction vary largely depending on the specific rifting episode as they are controlled by tectonic and magmatic activities (Sigmundsson 2006; Wright *et al.* 2012). Inter-rifting, co-rifting, and post-rifting phases are combined into a complete rifting episode (Sigmundsson 2006). A far field steady spreading that has good agreement with a new global plate motion 1A (NUVEL-1A) model is observed during inter-rifting phase, which is followed by a co-rifting phase (DeMets *et al.* 1994; Sigmundsson 2006; Pedersen *et al.* 2009). During the co-rifting phase, repeating dyke injections in the upper crust and extrusive activities often follow, releasing stresses and extensional strains that accumulated during the inter-rifting phase (e.g., Sigmundsson 2006, Wright *et al.* 2006; Pedersen *et al.* 2009), such as co-rifting phase at Askja (1920-1930) in Iceland (Sigurdsson & Sparks 1978), Asal-Ghoubbet (1978) in Djibouti (Vigny *et al.* 2007), and Dabbahu, Afar (2005-2010) in Ethiopia (Wright *et al.* 2012). A post-rifting phase follows the co-rifting phase where deformations near plate boundaries decrease gradually to the same extent as during typical inter-rifting phase (Hofton & Foulger 1996; Pollitz & Sacks 1996). However, the duration of a post-rifting phase can vary from a few years to a few decades, depending on the rheological responses within the tectonic setting. The variation of the post-rifting phase has been confirmed by Global Positioning System (GPS) observations that suggest that the duration of post-rifting relaxation for the co-rifting events at Krafla (1975–1984) in the Northern Volcanic Zone (NVZ) is a few decades (Fig. 2) (Árnadóttir *et al.* 2009; Pedersen *et al.* 2009).

1.1. Research aims

The main purpose of this research is to understand rheological response to inter-rifting phase and geodynamic process of the MAR system in Iceland. However, there are several particular objectives:

1. To estimate and understand pattern of surface deformation caused by tectonic and volcanic activities using GPS and precise leveling.
2. To develop an application for the most recent theory regarding the cooling of the oceanic lithosphere in modeling, particularly using Finite Element (FM) modeling.
3. To understand rheological responses to surface deformation caused by tectonic and volcanic activities.
4. To explore and estimate subsurface thermal conditions and viscosity beneath Iceland.

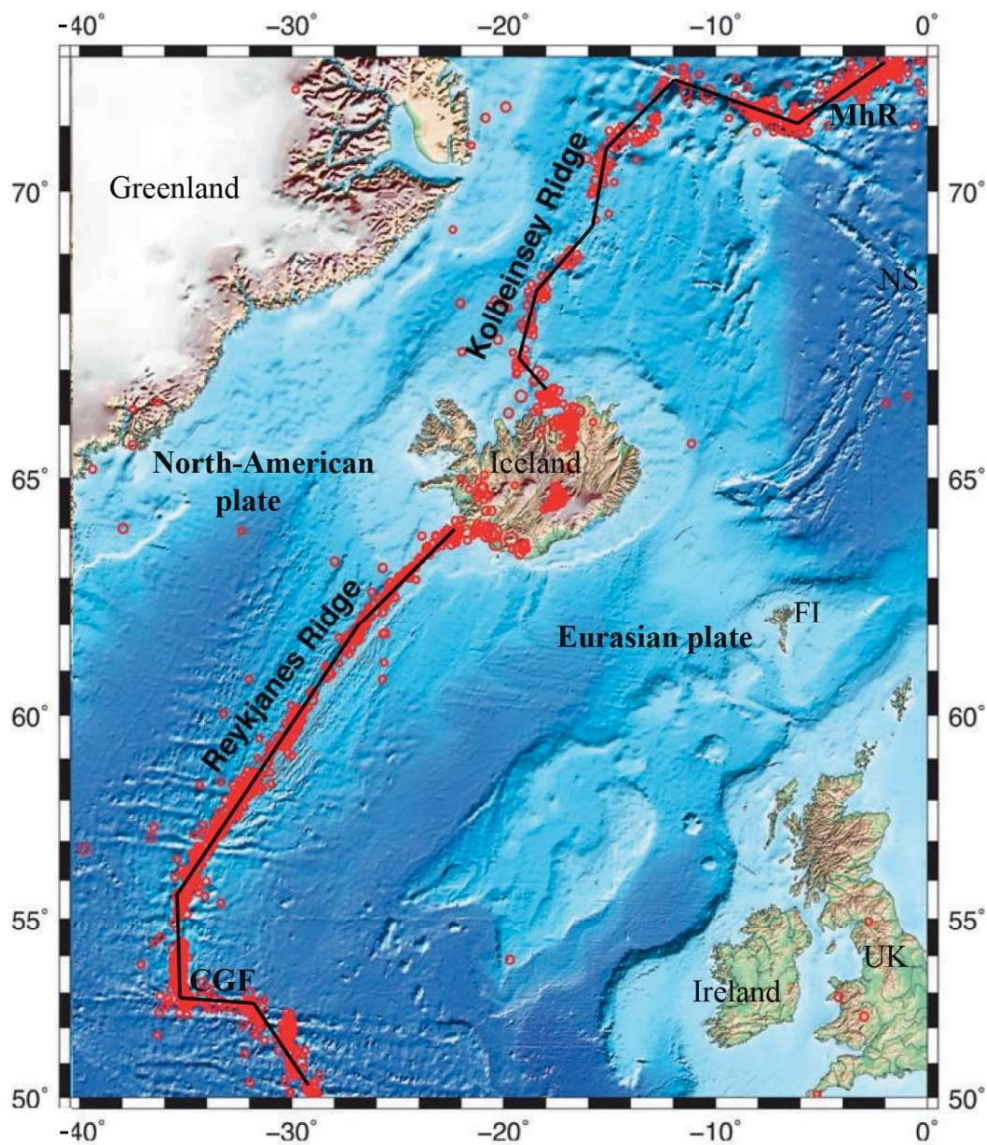


Figure 1. Plate boundaries of North-American and Eurasian plates in the Mid-Atlantic Ocean ridge. Black lines denote approximate plate boundaries. Red circles show location of epicenters of Earthquakes between 1964 and 2006. Charlie Gibbs Fracture Zone (CGF), Mohns Ridge (MhR), Faroe Islands (FI), Norwegian Sea (NS), and United Kingdom (UK) are also shown. This map is modification of Einarsson (2008).

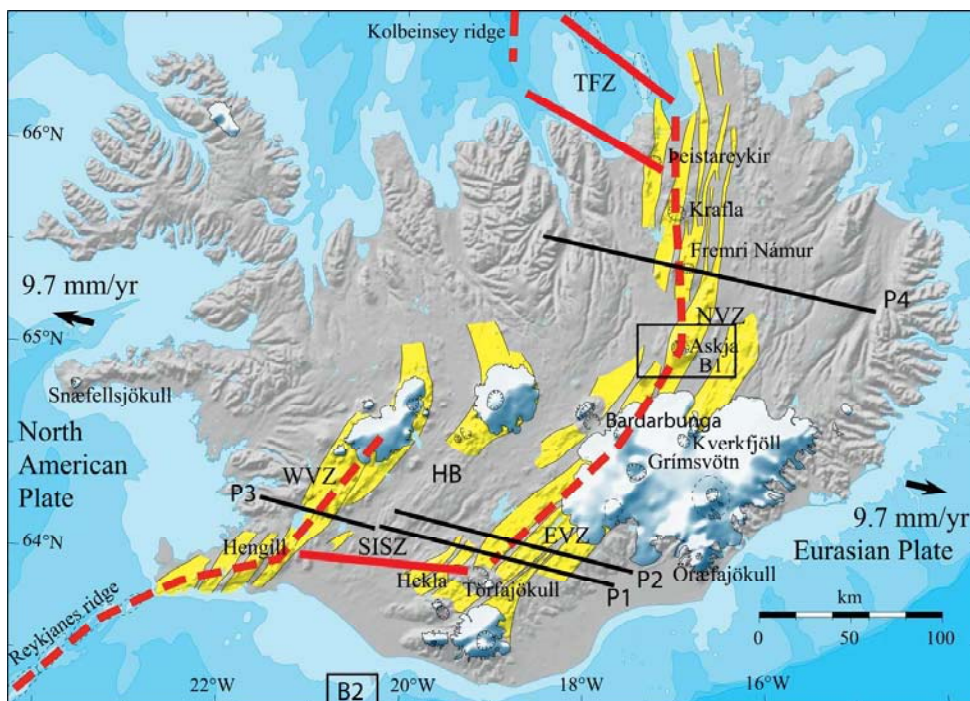


Figure 2. Plate boundary in Iceland. Red dashed lines show approximate central axis of plate boundaries. Red lines indicate two transform fault zones, e.g., South Icelandic Seismic Zone (SISZ) in the south and Tjörnes Fracture Zone (TFZ) in the north. The black vectors (far fields) indicate a relative plate spreading velocity between Eurasian and North American plates. Individual plate boundaries segments are indicated: Western Volcanic Zone (WVZ), Hreppar Block (HB), Eastern Volcanic Zone (EVZ), and Northern Volcanic Zone (NVZ). Fissure swarms (yellow) of individual volcanic systems are outlined. Major glaciers (white) are also shown. Location of profiles P1, P2, P3, and P4 for plate spreading deformations investigations are shown in Fig. 3. The box B1 for magmatic-tectonic (Askja) and the box B2 for volcanic activities are also shown in Fig. 4.

1.2. Study area: geology and tectonic settings

Iceland is mainly made of basalt (~92%). There are also ~4% basaltic andesites, ~1% andesites, and ~3% dacite-rhyolites (Jakobsson 1979). Tertiary rocks older than 3.3 Myr cover half of Iceland, with the oldest rocks (~16 Myr) found in northwest Iceland (Foulger 2006).

The crust beneath Iceland has been extensively investigated by seismic studies (e.g., Darbyshire *et al.* 2000; Kaban *et al.* 2002; Jones & MacLennan 2005; Bjarnason & Schemeling 2009). The Moho, the boundary between the crust and the mantle, lies from at a depth of ~20 km in the Krafla active rift area in the Northern Volcanic Zone (NVZ) to 29-km depth beneath central Iceland (Fig. 2) (Darbyshire *et al.* 2000). However, different authors have derived somewhat different conclusions on crustal thickness (see Sigmundsson 2006).

Previous models have used seismic and gravity data to determine the thermal structure beneath Iceland (e.g., Flóvenz & Sæmundsson 1993; Kaban *et al.* 2002; Björnsson 2008). The thermal gradient in the crust beneath Iceland varies greatly, from 0 to 500°C km⁻¹ (Flóvenz & Sæmundsson 1993). It is ~40-50°C km⁻¹ out of the flank zone (in the older rock), and it is

$\sim 150\text{--}200^\circ\text{C km}^{-1}$ in the flank zone of the active volcanic zone (Flóvenz & Sæmundsson 1993). Flank zones are characterized by volcanic activity that is not connected with the plate boundary. The two most important flanks are the Snæfellsjökull in the west and the Örfajökull in the east (Fig. 2). Different modelling approaches have resulted in somewhat different temperatures, from $\sim 600\text{--}800^\circ\text{C}$ (a thick crust model using a 20-40 km thick crust) to 1100°C (a thin crust model using a 10-15 km thick crust) (Flóvenz & Sæmundsson 1993; Sigmundsson 2006; Björnsson 2008). Similarly, Kaban et al. (2002) estimated the average depth of the 1200°C isotherm beneath central Iceland to be $\sim 30\text{--}50$ km, decreasing to ~ 20 km at the active central volcano (e.g., Krafla in the NVZ).

The divergent plate boundaries in Iceland can be detected by the active volcanism with exception of the flank zones (Fig. 2). The MAR system on Iceland is divided into the Western Volcanic Zone (WVZ), the Eastern Volcanic Zone (EVZ), and the NVZ (Fig. 2). These zones are characterized by central volcanoes and associated fissure swarms.

To address the objectives of the study, FE models are constrained by geodetic observations: (a) along four profiles – P1 and P2 in the EVZ, P3 in the WVZ, and P4 in the NVZ to study inter-rifting activities (Figs. 2 and 3), (b) at Askja (B1) in the NVZ to explore inter-rifting activities together with stacked shallow magma chamber at the plate boundaries (Figs. 2 and 4a), and (c) at Surtsey (B2) in southern Iceland, where Glacial Isostatic Adjustment and spreading are not believed to occur, to understand the load of a volcanic island on the crust (Figs. 2 and 4b).

In the EVZ, the profiles P1 and P2 are located between Torfajökull volcanic system and Vatnajökull glacier (Fig. 3a). The EVZ was activated $\sim 2\text{--}3$ Myr ago (Sæmundsson 1974) and propagates $\sim 35\text{--}50$ mm yr⁻¹ to the southwest (Einarsson 1991). The eastern and western parts of these profiles are located on the Eurasian plate and Hreppar block (a micro plate), respectively. The two profiles cross five parallel volcanic systems of a Postglacial lava field (<11 kyr), Upper Pleistocene (<0.8 Myr), and into the Plio-Pleistocene (0.8-3.3 Myr) (Jóhannesson & Sæmundsson 1998). In this area, the fissure swarms and faults follow a bearing of $N45^\circ\text{E}$ and are $\sim 30^\circ$ oblique to the spreading direction.

In the WVZ, profile P3 crosses Thingvellir rift graben in the north of Thingvallavatn in the WVZ (Fig. 3b). The WVZ was formed $\sim 7\text{--}9$ Myr ago when a rift jumped from the Snæfellsnes Peninsula (Fig. 2) to its present location (Sæmundsson 1992). This profile crosses at the center of the Thinvallahraun, Brunnar/Skógarkot, and Gjábakkahraun lava field, which erupted 9000-10,200 years ago and covers the tertiary lava in the west and Plio-Pleistocene in the east of the Thingvellir rift graben (Sinton *et al.* 2005). The Thingvellir graben consists of three major faults: Almannagja in the west and Hrafnagja and Bæjargja in the east (Paper 3). The eastern and western parts of this profile are located on the Hreppar block and North American plate, respectively. The Thingvellir graben is the northern extension of Hengill volcanic system and partly overlaps with Prestahnúkur volcanic system (Sinton *et al.* 2005). In this area, the faults and fissure swarms are directed to $\sim N30^\circ\text{E}$ (Guðmundsson 1987a) and are $\sim 15^\circ$ oblique to the plate motion normal direction. During the Holocene, the average subsidence of this graben floor is >35 m (Paper 3).

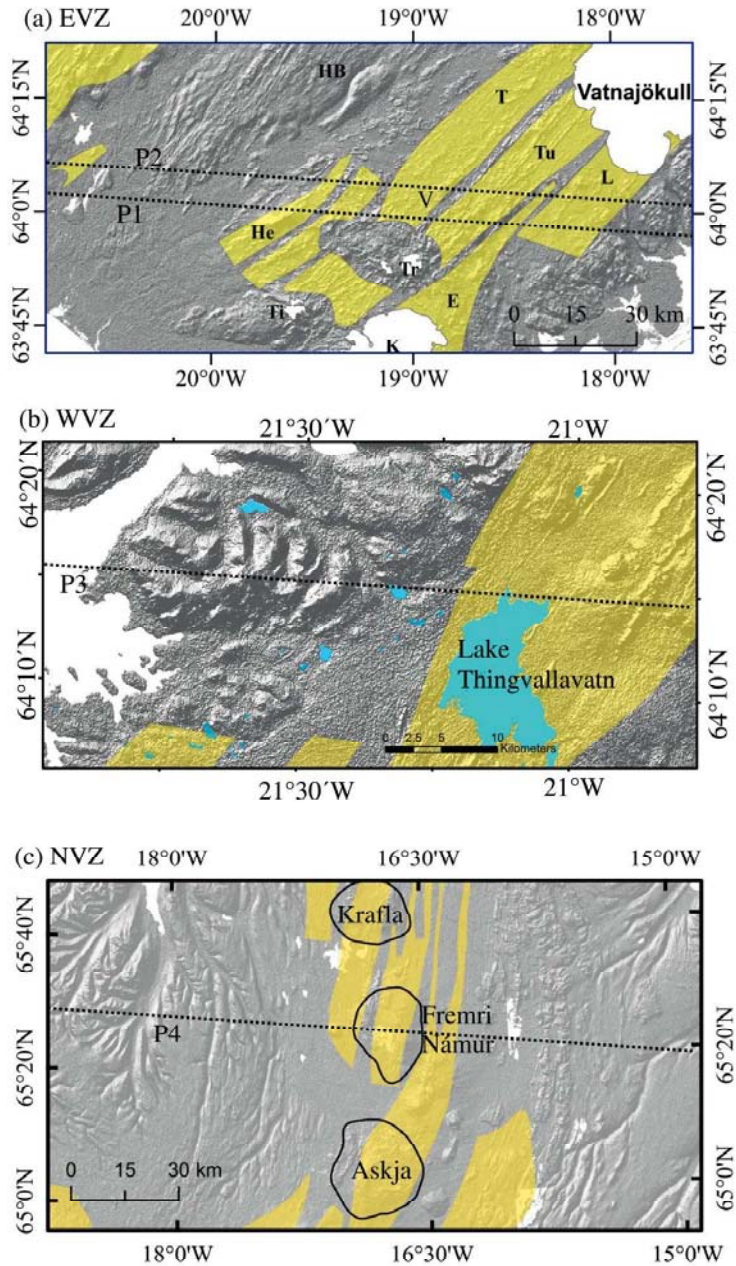


Figure 3. Location of profiles (P1-P4) in different volcanic rift zones investigated using rheological response to plate boundary deformation. Fissure swarms (yellow) of individual volcanic systems are outlined. (a) Eldgjá (E), Hekla (He), Hreppar block (HB), Katla (K), Torfajökull (Tr), Tindfjallajökull (Ti), Lakigigar (L), Torrlagigar (T), Tungna (Tu), and Vedifötn (V) are shown. (b) Water indicated by blue. (c) Central volcanoes are present by black polylines.

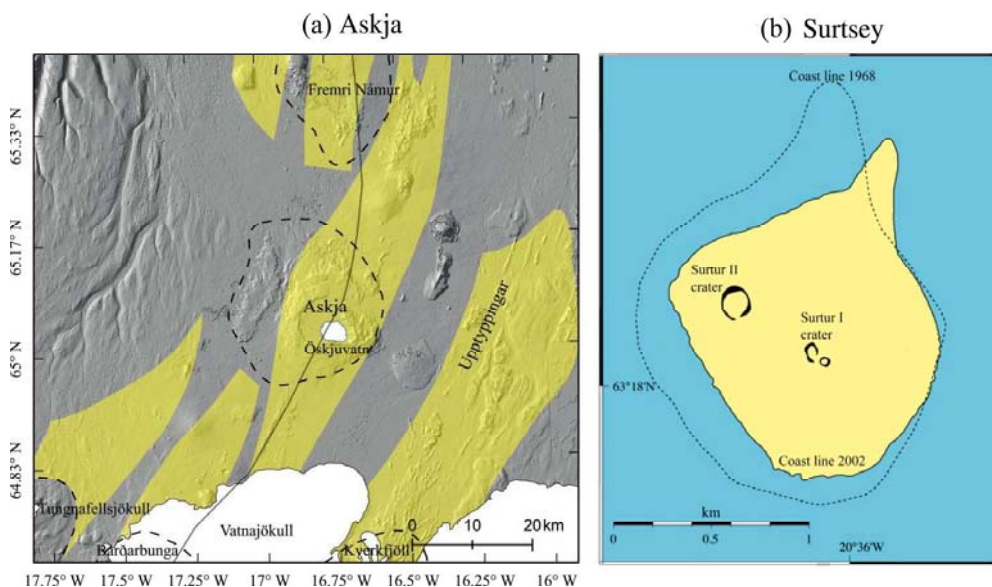


Figure 4. Detail location of (a) Askja and (b) Surtsey volcanic systems. (a) Fissure swarms of individual volcanic systems (yellow), location of central volcanos (black dashed lines), and approximate central axis of plate boundary (black polylines) are shown. (b) Surtsey volcanic island (yellow) and coast lines are also outlined.

In the NVZ, profile P4 crosses the Fremri Námur volcanic system between the Krafla and Askja volcanic systems (Figs. 2 and 3c). The NVZ was active ~6–7 Myr ago (Sæmundsson 1974). The NVZ consists of five volcanic systems arranged in an echelon with very little overlap (Fig. 1). According to NUVEL-1A, the normal spreading direction in this area is $N75^{\circ}W$. The faults and fissure swarms in the NVZ vary from $\sim N0-180^{\circ}E$; however, around the Fremri Námur volcanic system the orientation of major faults is $\sim N30^{\circ}E$ (i.e., 15° oblique to the normal plate spreading direction) (Fig. 3c) (Hjartardóttir 2013). The profile crosses the Postglacial lava field, Upper Pleistocene, Plio-Pleistocene, and Upper Tertiary (>3.3 Myr) (Jóhannesson & Sæmundsson 1998).

Volcano and volcano-tectonic interplay is studied at Askja volcanic system in the NVZ (Fig. 4a). A shallow magma chamber at ~ 3 -km depth at the plate boundary (e.g., Camitz *et al.* 1995; Sturkell & Sigmundsson 2000; Sturkell *et al.* 2006a; Pagli *et al.* 2006; de Zeeuw-van Dalfsen *et al.* 2012, 2013) and perhaps an elongated deeper source $\sim 16-20$ km (e.g., Sturkell *et al.* 2006a) are stretched by far field plate spreading. The Askja is located north of Vatnajökull and south of Fremri Namur volcanic system. Surtsey – a submarine volcanic system (now an Island) that was built by effusive activity between 1963 and 1967 in southern Iceland ~ 140 km from the mainland (Fig. 4b) (Moore *et al.* 1992) – has also been studied. Surtsey is assumed free of GIA and plate boundary deformations due to its geographical location (Fig. 2).

2. Surface deformations observations

Surface deformation caused by volcano-tectonic activities in Iceland have been studied since 1938, but with great intensity since 1960s with acceptance of the plate spreading model (e.g., Deckert *et al.* 1971, 1976; Gerke 1974; Tryggvason 1974, 1982, 1990; Brander *et al.* 1976; Heki *et al.* 1993; Sigmundsson *et al.* 1995; Jónsson *et al.* 1997; LaFemina *et al.* 2005;

Árnadóttir *et al.* 2006, 2009; Pedersen *et al.* 2009; Scheiber-Enslin *et al.* 2011; Geirsson *et al.* 2012). In 1938, researchers made the first attempt to estimate the width and depth of fissures (swarms) in the WVZ (Bernauer 1943). In addition, they setup the first triangulation network and leveling profile to investigate deformation field in the NVZ to confirm plate spreading (Niemczyk & Emschermann 1943). By assuming two stable end benchmarks along ~115 km profile in the NVZ, 4.8-m westward displacement of the center benchmark was estimated by re-measuring this triangulation network in 1965 (Tryggvason 1980). The widening between 1968 and 1972 of the Thingvellir graben (WVZ) was determined using Electronic Distance Measurements (EDM) (Brander *et al.* 1976), and the vertical displacement between 1967 and 1971 was estimated using precise leveling (Tryggvason 1974) (see Table 1 in Paper 4). The north section of Hekla of the EDM line in the EVZ shows a widening (1967-1970) and then contraction (1970-1973) (Decker *et al.* 1976).

However, space geodetic technique e.g., GPS was introduced country wide in the mid-1980s (e.g., Sigmundsson *et al.* 1995; Jónsson *et al.* 1997; LaFemina *et al.* 2005; Árnadóttir *et al.* 2006, 2009; Scheiber-Enslin *et al.* 2011; Geirsson *et al.* 2012). As of March 2016, a network with 90 continuous GPS stations (mostly in neo-volcanic zones in Iceland) has provided high resolution temporal and spatial data (available at <http://strokkur.raunvis.hi.is/gps/>). Furthermore, the Interferometric Synthetic Aperture Radar (InSAR) technique has been merged with GPS and revealed horizontal and vertical surface deformation with better resolution (e.g., Pagli *et al.* 2006, 2007; Pedersen *et al.* 2009; de Zeeuw-van Dalfsen *et al.* 2004, 2012, 2013).

Use of the early terrestrial techniques (e.g., triangulation, leveling, and EDM) combined with modern space geodetic techniques (e.g., GPS and InSAR) provide data that accurately and precisely reflect both temporal and spatial resolutions (see Einarsson *et al.* 2006; Sturkell *et al.* 2006b for more details). However, this research uses precise leveling (Paper 2; Paper 5; Manuscript in progress) and GPS data (Paper 1; Paper 2; Paper 3; Paper 4; Paper 5; Manuscript in progress).

2.1. Leveling data

Precise leveling are used to estimate subsidence at the center of a rift graben (Thingvellir rift graben in the WVZ), in Askja (tectonic-volcanic activities), and in Surtsey (an isolated volcanic system). Since 1966 (Eystein Tryggvason), leveling profiles in Iceland have been recorded. Since 1966, a leveling profile of ~8-km long crossing Thingvellir graben, north of Thingvallavatn in the WVZ, has been established and partly measured (along profile P3 in Fig 3b). The full measurement was continued in 1967, 1966, 1971, 1992, and 2007 (Tryggvason 1974, 1990; Paper 3). The new set of leveling data (1992-2007) together with previous data sets (1967-1971) provide maximum subsidence at the center of the rift graben of up to 1 mm yr⁻¹ relative to the first benchmark in the west (see Paper 3 for details). North of Askja a leveling measurement (1966-2015) with a profile ~1.7-km long bounded by two GPS stations reveals continuous subsidence and that the Askja volcanic system has been decaying exponentially at least since 1983 (Sturkell *et al.* 2006; Manuscript in progress). In Surtsey, the leveling data collected between 1991 and 2013 combined with previous data (1967-1991) (Tryggvason 1972; Moore *et al.* 1992; Sturkell *et al.* 2009) suggest that the subsidence is continuous but slowly decaying (Paper 5).

2.2. GPS data

Data collected using GPS are used to estimate deformation along the profiles: P1 (1994-2006) and P2 (2000-2010) crossing in the EVZ (Paper 1; Paper 2; Paper 4); P3 (1994-2010)

traverses Thingvellir rift graben in the WVZ (Paper 3); and P4 (2007-2013) crossing the NVZ (Paper 4) for inter-rifting activities and around Askja (2008-2013) for magmatic tectonic activities (Manuscript in progress) and at Surtsey (1992-2013) to test load of elastic plate (Paper 5).

To investigate plate spreading, the horizontal component of GPS data is projected onto profiles striking (e.g., N103°E for the WVZ, Paper 3) the approximate plate spreading direction of the plate motion model NUVEL-1A. Then spreading velocity along a profile is calculated using a formula from Savage & Burford (1973), who applied their formula to model a transform zone plate boundary. Vertical velocity is studied with reference to the International Terrestrial Reference Frame (ITRF) 1997, 2005, and 2008 (Boucher *et al.* 1999; Altamimi *et al.* 2007, 2012). The vertical deformation is affected by several processes – locally at central volcanos and GIA in a wider area. The need for GIA corrections has created some uncertainties.

3. Modeling

Elastic dislocation model (Fig. 5a) is applied widely to reproduce crustal deformation due to inter-rifting event of plate spreading in Iceland (e.g., LaFemina *et al.* 2005; Árnadóttir *et al.* 2006, 2009; Scheiber-Enslin *et al.* 2011; Geirsson *et al.* 2012) and elsewhere in the world (e.g., Apel *et al.* 2006; Saria *et al.* 2014). In this model, dykes move laterally with spreading velocity beneath a locking depth. This depth is called depth of elastic crust (LaFemina *et al.* 2005). Typically, Okada's formulas (1985) are used to calculate surface deformation. This model uses a pure elastic rheology that is an over simplification of Earth's rheology. Another set of stretching models (Fig. 5b) considers elastic and viscoelastic rheology (e.g., Berger 2004; Pedersen *et al.* 2009). Irrespective of the plate thickness (100 km) applied to stretching and rheological variation in both the lateral and vertical, this model is constrained to fit vertical surface deformations by ignoring style of horizontal deformations.

This study uses a temperature dependent rheological model that includes variations in the rheology away from the surface and the rift axis (Fig. 6) (Paper 1). In this model, only extensional stretching is applied to the lithosphere above the asthenosphere (Fig. 6b), although the thickness of lithosphere (20 km) is simplified to a fixed depth based on depths of the epicenters of earthquakes. A uniform thickness of the lithosphere is a clear short coming-

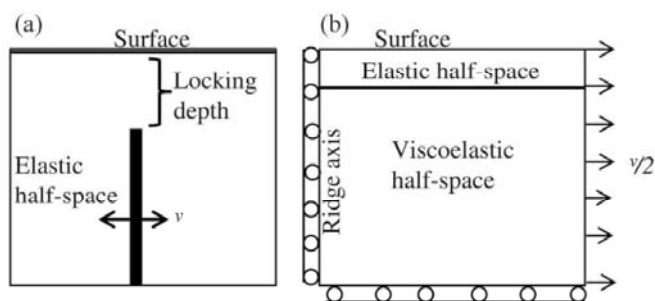


Figure 5. Model geometry applied to study inter-rifting event. (a) Elastic dislocation model where a dyke to the displacement, v , intrudes in the plate spreading direction under the locking depth (more details at Fig. 10 in LaFemina *et al.* 2005, p. 13). (b) A stretching model where far field (the farthest right) is stretched by spreading velocity, v . The vertical left and bottom boundary can move vertically and horizontally, respectively, but is fixed in the other direction (more details at Fig. 5 in Pedersen *et al.* 2009, p. 20).

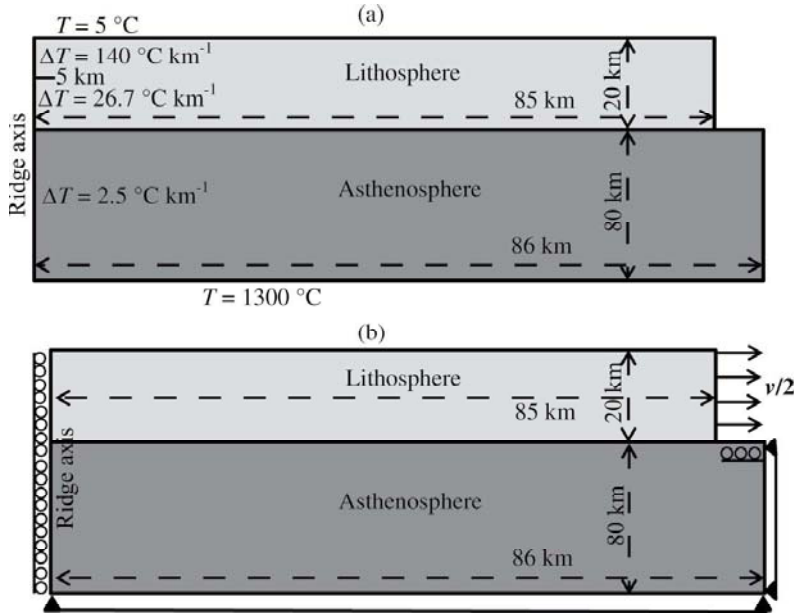


Figure 6. Geometry and boundary conditions of thermo-mechanical stretching model: (a) thermal boundary conditions and (b) mechanical boundary conditions where far field of lithosphere is stretched by spreading velocity, v . The ridge axis is fixed laterally but can move vertically. Bottom and right boundaries of asthenosphere are fixed. The surface (most upper boundary) is free to move any direction (more details in Paper 1). The figure is not to scale.

since the lithospheric thickness increases with distance from rift and surface. This model stretches the lithosphere above the asthenosphere that was identified by a particular isotherm (700°C) (Fig. 7) (Paper 3). This approach is more realistic as the model takes into account the most recent theory of the cooling of the oceanic lithosphere. This model is further applied to study subsurface mass flow patterns (Paper 2), to understand the rheological response on surface deformation in the EVZ and the NVZ (Paper 4), and to understand magmatic and tectonic activities in Askja in the NVZ (Manuscript in progress). However, to study the lithospheric load on the Surtsey volcanic system, which is far away from GIA and plate boundary deformation zones, a uniform Newtonian rheology is applied (Paper 5).

3.1 Rheology in modeling

To reproduce tectonic and volcano-tectonic deformation, we used a temperature and stress-dependent creep power law (Paper 1; Paper 3; Paper 4; Manuscript in progress), temperature-dependent Newtonian rheology (Paper 2), and a uniform rheology with viscosity $3\text{-}5 \times 10^{18}$ Pa s (Paper 5) for all models. The temperature framework considers a) excess temperature ($100\text{-}200^{\circ}\text{C}$) caused by the plume beneath Iceland (MacLennan *et al.* 2001; Ruedas *et al.* 2004; Sigmundsson 2006; Schmeling & Marquart 2008), the mantle temperature (1400°C) for a normal MOR (Turcotte & Schubert 2002), and a temperature between 1410 and 1760°C for the phase transition to an olivine-spinel environment at the base of the asthenosphere (Morishima *et al.* 1994). The creep power law can be described mathematically in relation to strain rate ($\dot{\epsilon}$) with absolute temperature (T) (K) and differential stress (σ) (MPa):

$$\dot{\epsilon} = A\sigma^n d^{-i} C_{HO}^r e^{-\frac{E_a + PV}{RT}}, \quad (1)$$

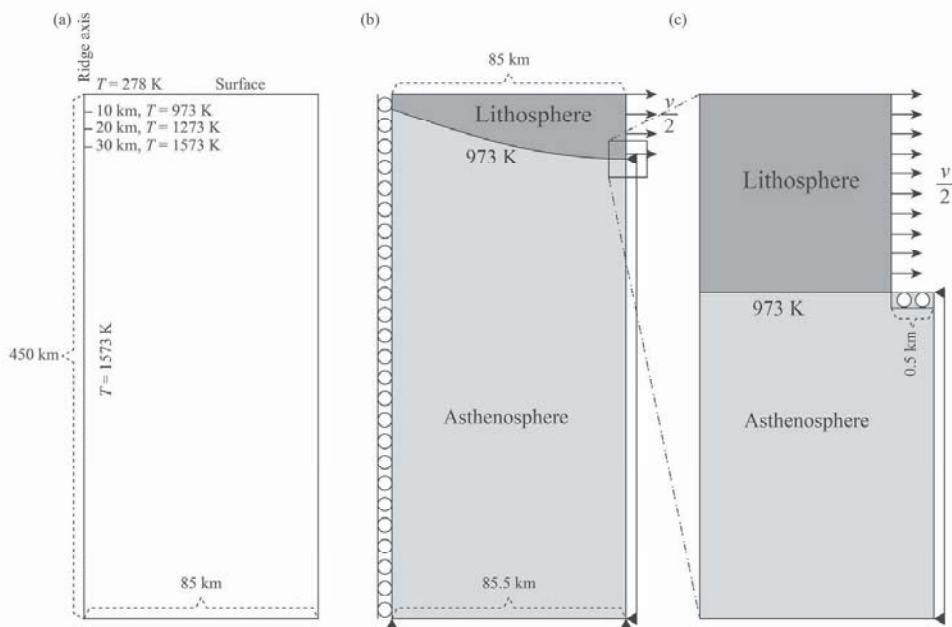


Figure 7. Geometry and boundary conditions of the thermo-mechanical stretching model: (a) thermal boundary conditions and (b) lithosphere and asthenosphere boundary defined by the 700°C (973K) isotherm. Mechanical boundary conditions: the far field of lithosphere is stretched by spreading velocity, v . The ridge axis is fixed laterally but can move vertically. Bottom and right boundaries of asthenosphere are fixed. The surface (upper most boundary) is free to move any direction (more details at Fig. 6 in Paper 3). The figure is not to scale.

where A is pre-exponential factor and often used as scale factor, n is exponent of σ , d (μm) is grain size and i is its exponent, C_{HO} ($\text{H}/10^6\text{Si}$) is water component and r is its exponent, E_a (kJ mol^{-1}) is activation energy, P (GPa) is pressure, V ($10^{-6} \text{ m}^3 \text{ mol}^{-1}$) is activation volume, and R ($\text{J mol}^{-1} \text{ K}^{-1}$) is universal gas constant (e.g., Karato 1997; Hirth *et al.* 2001; Korenaga & Karato 2008; Freed *et al.* 2010). The creep law can be applicable in three ways: 1) diffusion creep, a strain rate that is linear to the applied stress ($n = 1$), i.e., a linear rheology; 2) dislocation creep, a strain rate that is not linear to the applied stress ($n = 3-6$), i.e., a non-linear rheology; and 3) composite creep, a situation that combines the effect of diffusion and dislocation creep, i.e., a diffusion and dislocation rheology. Dislocation creep flow is independent of grain size. How these creeps respond depends on water content – wet (0.03% water saturated) and dry (completely water free) conditions (Karato & Wu 1993).

In both wet and dry conditions, dislocation creeps are applied preliminary to reproduce the surface deformation in the EVZ (Paper 1). Based on the results in Paper 1, only a dry dislocation creep is applied in the Thingvellir rift graben in the WVZ (Paper 3). Furthermore, diffusion, dislocation, and composite creep flows in both wet and dry conditions are used to study rheological responses on deformation in the EVZ and the NVZ (Paper 4). To study subsurface mass flow pattern due to plate spreading and corresponding surface deformation, a temperature-dependent Newtonian rheology is used (Paper 2). Based on previous results and modeling, a dry dislocation creep flow is used to study the interplay between volcano and

tectonic activities in the Askja volcanic system (Manuscript in progress). The Surtsey volcanic system, however, is out of active rift zone, so horizontal and vertical variations of rheological properties are not assumed to be significantly different in shallow depths. In addition, a uniform rheology with viscosity of $3\text{-}5 \times 10^{18}$ Pa s is applied to understand lithostatic load of the erupted material (Paper 5).

4. Results and Discussion

Geodetic GPS observations show individual spreading velocities (Tab. 1) along respective profiles in Iceland, velocities that are very similar to previous measurements (e.g., LaFemina *et al.* 2005; Árnadóttir *et al.* 2009; Scheiber-Enslin *et al.* 2011; Geirsson *et al.* 2012), plate motion models (e.g., NUVEL-1A, Mid-Ocean Ridge VELOCITY 2010) (MORVEL2010) (DeMets *et al.* 2010), and REcent plate VELOCities 2000 (REVEL2000) (Sella *et al.* 2002)).

Similarly, deformation zones crossing a plate boundary in different volcanic zones with different geometry are also fairly similar (e.g., Camitz *et al.* 1995; Hofton & Foulger 1996) and agree with our previous findings (e.g., Paper 1; Paper 2; Paper 4). The deformation zone in the EVZ is wider (100-km crossing rift) compared with the NVZ and WVZ (Fig. 8; Tab. 1). The profiles (P1 and P2) in the EVZ cross five parallel volcanic systems (north of Torfajökull and south of Vatnajökull), where deformation is distributed over that wider area (Figs. 3a and 8b). In the EVZ, there is no prominent geothermal system in the study area and a subsurface thermal system penetrates five parallel volcanic systems, making this area comparatively cooler (up to $\sim 54^\circ\text{C km}^{-1}$) than the NVZ and the WVZ (Figs. 3 and 8; Tab. 1). Therefore, the shape of the 700°C isotherm is a bit flatter and is at 13-km depth at the ridge axis. Deformations are linked with the subsurface thermal distribution and high thermal activity initiates more surface deformation (Buck *et al.* 2005; Behn & Ito 2008). The flatter shape and the comparatively thicker crust (by 700°C) in the EVZ results in a wider deformation zone (Fig. 8b) but fewer deformations. The deformation zone in the WVZ is narrower than in the EVZ. The profile P3 in the WVZ crosses two overlapping volcanic systems north of Lake Thingvallavatn (Figs. 3b and 8a). Along this profile, the thermal gradient at the ridge axis is $\sim 87.5^\circ\text{C km}^{-1}$; this temperature is higher than in the EVZ but lower than in the NVZ. This lower temperature may be due to the cooling effect of circulating water from Lake Thingvallavatn and most importantly the fact that the prominent geothermal system (Hengill) is farther away (south of Lake Thingvallavatn) from the study area (Figs. 2, 3b and 8a). In the WVZ, the shape of this isotherm is comparatively steeper than in the EVZ and the depth of this isotherm is 8 km at the ridge axis. The deformation zone in the NVZ is the narrowest (58 km crossing rift) compared with the EVZ and the WVZ if plate stretching is taken into consideration (Fig. 8; Tab. 1). This difference is likely an effect of the geometrical relation with the neighboring volcanic systems and geothermal activities. The profile (P4) in the NVZ crosses one major volcanic system among five en-echelon volcanic systems, where deformation is concentrated to that particular volcanic system (Figs. 3c and 8c). The thermal systems concentrate in a single volcanic system in the NVZ due to geometrical arrangement of volcanic systems in the north. The profile P4 in the NVZ crosses an active geothermal area, which leads to a high thermal gradient up to $\sim 117^\circ\text{C km}^{-1}$ and a steep cone shape for the 700°C isotherm (Figs. 3c and 8c). Therefore, the width of the thinnest crust (defined by 700°C) is narrow where there are many deformations (Fig. 8). In the neighbouring volcanic system to the south, the shallow magma chamber (3.5 km) under Askja at the plate boundary in the NVZ further pushes the 700°C isotherm to a depth as shallow as 2 km (Fig. 9).

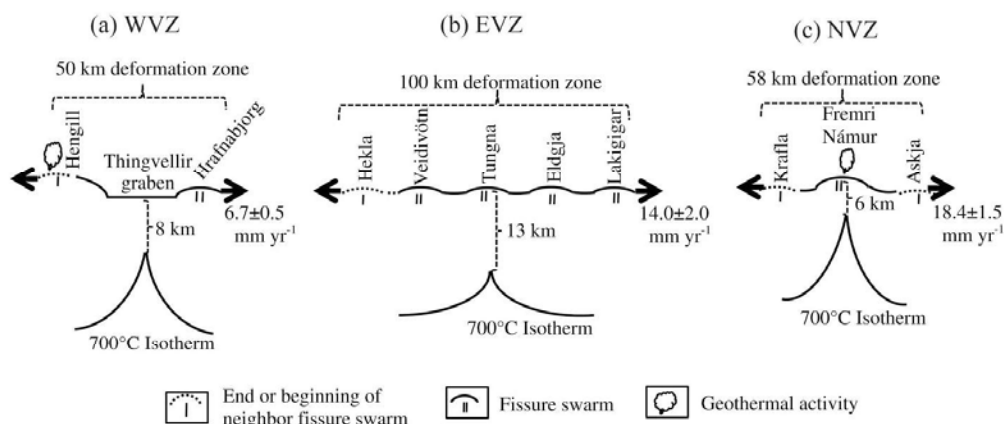


Figure 8. Schematic view of east-west cross sections of different volcanic rift zones in Iceland. The figure is not to scale.

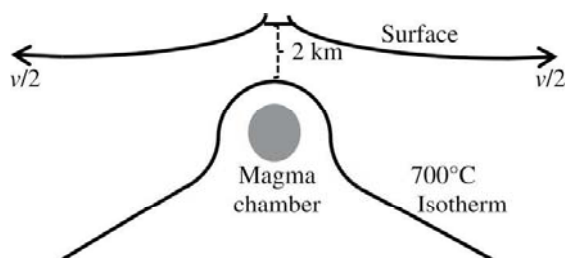


Figure 9. Schematic view of east-west cross section of Askja volcano. Here v is spreading velocity. The figure is not to scale.

Here we refer to the depth of the 700°C isotherm at the ridge axis as the boundary of the brittle-ductile transition, as the rheology beneath Iceland is comparable to the deformation evident observed during laboratory experiments of olivine rheology (Turcotte & Schubert 2002; Kaban *et al.* 2002; Sigmundsson 2006; Björnsson 2008; Schmeling & Marquart 2008; Jakobsdóttir 2008; Paper 3; Paper 4). The depth to the brittle-ductile transition is fairly similar with those identified as locking depth by an elastic dislocation model (e.g., LaFemina *et al.* 2005; Árnadóttir *et al.* 2009; Scheiber-Enslin *et al.* 2011; Geirsson *et al.* 2012), the focal depth of epicentres of shallow earthquakes (Stefánsson *et al.* 1993; Jakobsdóttir 2008; Soosalu *et al.* 2010; Key *et al.* 2011; White *et al.* 2011), the depth of dyking (Sigmundsson *et al.* 2015), and the upper middle crustal thickness (Bjarnason & Schmeling 2009).

The results from the models give a thermal gradient (ΔT) from the 700°C isotherm to the surface at the ridge axis. This ΔT is compared with Pálmason & Sæmundsson (1979) and Flóvenz & Sæmundsson (1993) who suggested that the location of profiles in the EVZ (P1 and P2) and WVZ (P3) are neither on the flank of the active volcanic zone nor on the oldest rock. The location of the profiles may have resulted in the arrangement of the volcanic systems and the geothermally active areas (Fig. 8; Tab. 1). The ΔT in the EVZ is fairly similar with the ΔT at the ridge axis of the MOR, whereas it is two to three times higher in the WVZ and the NVZ than in the MOR. However, very few thermal studies have been conducted at neo-volcanic zones in Iceland, so there is a lack of data to compare the ΔT in this study. The

Table 1. Similarities and dissimilarities among volcanic zones.

Parameters	WVZ	EVZ	NVZ
Rift zone	Two parallel rifts (shared by the EVZ)	Two parallel rifts (shared by the WVZ)	A single rift
Spreading velocity (mm yr^{-1})	6.7 ± 0.5 (~35%)	14.0 ± 2.0 (~75%)	18.4 ± 1.5 (100%)
Width of deformation zone (85%-90%) crossing rift (km)	~50	~100	~56
Rift and subsidence centers	Approximately same location	Subsidence center is ~8 km east of rift center	Approximately same location
Deformation system	Controlled by volcanic systems	Controlled by volcanic systems	Controlled by volcanic systems
Deformation next to the rift is dominated by	Dislocation creep	Dislocation creep	Dislocation creep
Geometry of volcanic systems	Two overlapping volcanic systems	Five parallel volcanic systems	Five <i>en-echelon</i> volcanic systems
Studied profiles	Crossing relatively hot surface next to geothermal area	Crossing cold surface with five parallel volcanic systems	Crossing geothermally hot surface with one major volcanic system (Fremri námur)
Thermal system of the geometry of 700°C isotherm	Concentrate individual volcanic systems	Distributed among the volcanic systems	Concentrate individual volcanic systems (Fremri námur)
Depth of the 700°C isotherm at the ridge axis (km)	8	13	6
Thermal gradient above the 700°C isotherm at the ridge axis ($^{\circ}\text{C km}^{-1}$)	~87.5	~54	~117

uppermost few hundred meters of crust in the active rift zones are highly fractured and cut by several faults systems (Fig. 2). Due to cold water circulation, no difference in temperature is found up to 1-km depth (Björnsson *et al.* 2005, p. 671). However, the ΔT at different zones in this research is higher than ΔT in the older rock ($40\text{-}50^{\circ}\text{C km}^{-1}$) (Flóvenz & Sæmundsson 1993).

In models that include the most bottom boundary as locked, the influx of materials into the model cannot take place. Therefore, vertical subsidence is expected within 30 to 40 km from the rift axis (Paper 4), a finding that is comparable to Pollitz & Sacks (1996) who suggested that a similar width of a vertical deformation zone was due to tectonic loading in the NVZ. However, subsidence caused by plate stretching in the NVZ is mostly leveled up by magmatic activities if the GIA correction is considered. This is comparable to the Afar in Ethiopia (Pagli *et al.* 2014) and at the Asal-Ghoubbet rift in Djibouti (Cattin *et al.* 2005). On the other hand, fault geometry (asymmetric) of the Thingvellir rift graben (WVZ) in the ultra-slow spreading segment of the MAR suggests that magmatic activities make this graben alive (Sæmundsson 1992; Dick *et al.* 2003; Buck *et al.* 2005; Behn & Ito 2008), although magmatic influx is not

sufficient to level up the subsidence caused by plate stretching (Paper 3). The boundary faults in this graben correlate well with the shallow depth of the 700°C isotherm in the model (Paper 3). In the EVZ, the eastern and western parts of the profiles are dominated by subsidence and uplift, respectively (Paper 1; Paper 2; Paper 4). However, to reproduce the observed style of vertical deformation in the EVZ at 100-km depth, the highest magmatic influx of $\sim 11 \text{ mm yr}^{-1}$ takes place $\sim 10\text{-}20 \text{ km}$ west of the rift center (Paper 2). The rift centre is defined by the center of horizontal deformations. Geodetic observations and model results suggest that the subsidence center in the EVZ is $\sim 8\text{-}10 \text{ km}$ east of the spreading centre (Paper 2; Paper 4). This situation is also observed in Djibouti at the Asal-Ghoubbet rift (Cattin *et al.* 2005). In the WVZ and the NVZ, the spreading and the subsidence centers are approximately in the same location (Paper 3; Paper 4).

In this study, dislocation, diffusion, and composite creep rheology with both wet and dry conditions are investigated and evaluated. A model of dislocation and composite creep resulted in observed style tangential horizontal displacement, whereas a model of diffusion creep resulted in a liner pattern of horizontal deformation (Paper 4). Furthermore, the composite creep model requires a relatively shallow depth of the 700°C isotherm at the ridge axis. This attributes to hotter conditions at shallow depths and in this condition dislocation creep is more appropriate (Paper 1; Paper 4). On the other hand, the results of wet and dry rheological models do not differ significantly (Paper 1; Paper 4). Reproduced rheological behavior in the models suggests that close to the rift axis beneath Iceland deformation is dominated by dry dislocation rheology.

A model that used dislocation creep flow in dry conditions resulted in better fit for a volcano at the plate boundary (e.g., the Askja) (Manuscript in progress). Different models evaluated different magma chamber geometries. A model using an oblate ellipsoidal ($2 \times 0.5 \text{ km}$) source at 3.5-km depth (cf., Pagli *et al.* 2006) reproduced $\sim 4 \text{ mm yr}^{-1}$ higher subsidence than observations ($\sim 30 \text{ mm yr}^{-1}$) due to solidifications of magma in the magma chamber even though spherical or prolate ellipsoidal shape of magma chamber is suggested to be present at a slow spreading divergent plate boundary, which is likely in Krafla (Tryggvason 1980; Gudmundsson 1986, 1987b; Dick *et al.* 2003). Elastic Mogi single and double sources ($\sim 15\text{-}18 \text{ mm yr}^{-1}$), Penny ($\sim 14 \text{ mm yr}^{-1}$), Spherical ($\sim 14 \text{ mm yr}^{-1}$), and Ellipsoidal ($\sim 17 \text{ mm yr}^{-1}$) reproduced about half of observed subsidence. Combined effect of volcano-tectonic activities resulted $\sim 15 \text{ mm yr}^{-1}$ higher subsidence at the center than observation (Manuscript in progress). This higher subsidence may be the effect of high subsurface temperature at a shallow depth of stretching. Tectonic, volcanic, and GIA studies in Iceland suggest, however, a uniform viscosity of both $< 5 \times 10^{18} \text{ Pa s}$ (Sjöberg *et al.* 2004; Fleming *et al.* 2007; Jacoby *et al.* 2009) and $> 5 \times 10^{18} \text{ Pa s}$ (Sigmundsson & Einarsson 1992; Wolf *et al.* 1997; LaFemina *et al.* 2005; Árnadóttir *et al.* 2009; Auriac *et al.* 2013), viscosities that indicate wet and dry rheology, respectively (Barnhoorn *et al.* 2011).

In this study, a uniform viscosity of $3 \times 10^{18} \text{ Pa s}$ for asthenosphere beneath Surtsey is constrained from lithostatic load that has depressed the surface of 27.5 cm over 50 years by a 50 km (by 700°C isotherm in Paper 4) average depth of lithosphere (Paper 5). This viscosity is fairly similar to what others have found (e.g., Fleming *et al.* 2007; Jacoby *et al.* 2009).

The 700°C isotherm shows good correlation with its shallow depth in the model and for the width of Thingvallir rift graben faults (WVZ) (Paper 3). In Askja, along with the plate spreading, a shallow magma chamber (3.5 km) pushes the location of the 700°C isotherm to a shallower depth (2 km) (Fig. 9) (Manuscript in progress).

5. Conclusion

The main conclusions of this study are summarized as followings:

- At Surtsey, the subsidence rate is decaying, from $\sim 10 \text{ mm yr}^{-1}$ between 1992 and 2000 to $\sim 8 \text{ mm yr}^{-1}$ between 2000 and 2002, to $\sim 3 \text{ mm yr}^{-1}$ between 2002 and 2013. This decrease seems to be caused by lithostatic loading of the erupted material and compaction of the volcanogenic material ($\sim 0.02\%$). A 50-km thick lithospheric model considering the asthenosphere with a uniform viscosity of $3 \times 10^{18} \text{ Pa s}$ results in 27.5 cm subsidence due to the load of eruptive materials.
- The divergent spreading velocity of MAR segments in Iceland is estimated to be 6.7 ± 0.5 (WVZ), 14.0 ± 2.0 (EVZ), and 18.4 ± 1.5 (NVZ) mm yr^{-1} . The deformation zones are estimated to be ~ 50 , ~ 100 , and $\sim 58 \text{ km}$ for the WVZ, EVZ, and the NVZ, respectively, crossing the rift axis that accommodates $\sim 85\text{-}90\%$ of the deformations.
- Dry rheological models provide slightly better results than wet models, but the models do not differ significantly. Dominant deformation in the rift zone in Iceland is governed by dislocation creep. To account for the observed surface deformation in the EVZ, a maximum magmatic influx of $\sim 11 \text{ mm yr}^{-1}$ at 100-km depth is estimated to be $\sim 10\text{-}20 \text{ km}$ west of the rift center.
- The depths of the 700°C isotherm at the ridge axis are different in the EVZ (13 km), WVZ (8 km), and the NVZ (6 km). The thermal gradient above the isotherm is similar between the EVZ and the MOR, but it is $\sim 2\text{-}3$ times higher in the WVZ and the NVZ than in the MOR. However, a shallow magma chamber (3.5 km) at Askja pushes the 700°C isotherm even shallower ($\sim 2 \text{ km}$).
- At Askja, the model results in $\sim 4 \text{ mm yr}^{-1}$ higher subsidence ($\sim 34 \text{ mm yr}^{-1}$) than what is observed ($\sim 30 \text{ mm yr}^{-1}$) because of solidification of magma in the magma chamber. However, a model for volcano-tectonic interplay at Askja generates $\sim 15 \text{ mm yr}^{-1}$ subsidence ($\sim 54 \text{ mm yr}^{-1}$) higher than expected ($\sim 39 \text{ mm yr}^{-1}$).
- In the EVZ and the NVZ, the depth of estimated viscosity of $5 \times 10^{18} \text{ Pa s}$ by thermo-mechanical model at the ridge axis is 12 and 7 km, respectively.
- A uniform rheological model may provide sufficiently reasonable understanding for an isolated (from rift) volcanic system (Surtsey). However, in the active rift zone in Iceland, the thermo-mechanical geodynamic micro models are strongly suggested and this provides insight into subsurface strain-stress relationships caused by tectono-volcanic activities.

Future work

To investigate a cross-section crossing a rift zone and/or a volcano-tectonic interplay (e.g., Askja, Krafla), a 2D FE thermo-mechanical model should suffice. However, in a wider context, 3D FE thermo-mechanical model is suggested where a) a latitude dependent spreading velocity can be applied and b) different directions ($0\text{-}90^\circ$) of tectono-volcanic arrangement can be simulated. Furthermore, to understand the wide range of rheological responses in Iceland, a 3D thermo-mechanical model should consider at least three components (e.g., plate spreading, volcano deformation, and GIA), a strategy used for studying such as for the Grímsvotn volcanic system.

Acknowledgement

First of all, I am the most thankful to Almighty **Allah (su)** who bestows His blessings not only for this thesis work but for all my life. He is the one who made me capable to complete this study.

I gratefully acknowledge my supervisor Prof. Erik Sturkell for all his support during this study. His continuous supervision made it easy to go into greater deep in this study. His patience makes me comfortable. Thanks, Erik, for sharing your gathered experiences and knowledge. I am thankful to co-supervisor Dr. Freysteinn Sigmundsson, who has extensive knowledge on geodynamics in Iceland, for helping with both ideas and technical support during my time at the Iceland University. I am also grateful to examiner Prof. Rodney Stevens who provided timely updates and provided constructive comments that helped improve the qualitative research. I would also like to thank to Prof. Björn Lund as well as Dr. Peter Schmidt for their fruitful discussions and technical support during my time at Uppsala University.

I want to thank to my friends and colleagues at the University of Gothenburg, Iceland University, and Uppsala University for their technical support, their knowledge, and their happy attitude. All of this made research enjoyable. I am thankful to Dr. Gabrielle Stockmann for the support, including nice food at different restaurants and providing me with a place to stay while time in Reykjavik, Iceland.

I also gratefully acknowledge financial support from Herbert and Karin Jacobssons Stiftelse, Knut and Alice Wallenbergs Stiftelse, Paul and Marie Berghaus, and Sven Lindqvist's Research Foundation for travel grants for my field work, meetings, and conferences.

It is the ultimate output of my mother's hard input in my early life. My father would be very happy if he was in the world today. My brothers and sister have always been encouraging and unconditionally supportive. My happy world is my daughter Tahiyat Rabab. Alhamdulillah, we always go through a joyful time! Ever since 30th December 2007, my wife, Mosammath Romena Khatun, has always been with me and kept me focused on my work. This thesis is the output of all their efforts with and for me. May Allah give us the guidance and best rewards here and hereafter.

References

- Altamimi, Z., Collilieux, X., Legrand, J., Garayt, B. & Boucher, C., 2007. ITRF2005: A new release of the International Terrestrial Reference Frame based on time series of station positions and Earth Orientation Parameters, *J. Geophys. Res.*, **112**(B09401), 1-19, doi:10.1029/2007JB004949.
- Altamimi, Z., Métivier, L. & Collilieux, X., 2012. ITRF2008 plate motion model, *J. Geophys. Res.*, **117**(B07402), 1-14, doi:10.1029/2011JB008930.
- Apel, E.V., Bürgmann, R., Steblov, G., Vasilenko, N., King, R. & Prytkov, A., 2006. Independent active microplate tectonics of northeast Asia from GPS velocities and block modeling, *Geophys. Res. Lett.*, **33**(L11303), 1-5, doi:10.1029/2006GL026077.
- Árnadóttir, T., Jiang, W., Feigl, K.L., Geirsson, H. & Sturkell, E., 2006. Kinematic models of plate boundary deformation in southwest Iceland derived from GPS observation, *J. Geophys. Res.*, **111**(B07402), 1-16, doi:10.1029/2005JB003907.
- Árnadóttir, T., Lund, B., Jiang, W., Geirsson, H., Björnsson, H., Einarsson, P. & Sigurdsson, T., 2009. Glacial rebound and plate spreading: results from the first countrywide GPS observations in Iceland, *Geophys. J. Int.*, **177**, 691-716, doi:10.1111/j.1365-246X.2008.04059.x.
- Auriac, A., Spaans, K.H., Sigmundsson, F., Hooper, A., Schmidt, P. & Lund, B., 2013. Iceland rising: Solid Earth response to ice retreat inferred from satellite radar interferometry and viscoelastic modeling, *J.*

- Geophys. Res.*, **118**(4), 1331-1344. doi:10.1002/jgrb.50082.
- Barnhoorn, A., van der Wal, W. & Drury, M.R., 2011. Upper mantle viscosity and lithospheric thickness under Iceland, *J. Geodynamics*, **52**, 260-270, doi:10.1016/j.jog.2011.01.002.
- Behn M.D., & Ito, G., 2008. Magmatic and tectonic extension at mid-ocean ridges: 1. Controls on fault characteristics, *Geochem. Geophys. Geosys. G³*, **9**(8), 1-22, doi:10.1029/2008GC001965.
- Berger, A., 2004. Crises volcano-tectoniques et divergence de plaques en Islande: Mesure par GPS et modelisation numerique, *PhD thesis*, Applied geology, Université de Savoie, French.
- Bernauer, V.F., 1943. Junge Tektonik auf Island und ihre Ursachen, in *Spalten auf Island*, pp. 14-64, ed. Niemczyk, O., Verlag Von Konrad Wittwer, Stuttgart, Germany.
- Bjarnason, I.T. & Schmeling, H., 2009. The lithosphere and asthenosphere of the Iceland hotspot from surface waves, *Geophys. J. Int.*, **178**, 394-418, doi:10.1111/j.1365-246X.2009.04155.x.
- Björnsson, A., 2008. Temperature of the Icelandic crust: inferred from electrical conductivity, temperature gradient, and maximum depth of earthquakes, *Tectonophysics*, **447**, 136-141, doi:10.1016/j.tecto.2006.02.027.
- Björnsson, A., Eysteinnsson, H. & Beblo, M., 2005. Crustal formation and magma genesis beneath Iceland, in *Plates, Plumes, and Paradigms*, pp. 665-686, ed. Foulger, G.R., Natland, J.H., Presnall, D.C. & Anderson, D. L., The Geological Society of America, Spatial Volume 388.
- Boucher, C., Altamimi, Z. & Sillard, P., 1999. *The 1997 International Terrestrial Reference Frame (ITRF-97)*, Obs. De Paris, Paris.
- Brander, J.L., Mason, R.G., & Calvert, R.W., 1976. Precise distance measurements in Iceland, *Tectonophysics*, **31**(3-4), 193-206.
- Buck, W.R., Lavier, L.L. & Poliakov, N.B., 2005. Modes of faulting at mid-oceanic ridges, *Nature*, **434**, 719-723.
- Camitz, J., Sigmundsson, F., Foulger, G., Jahn, C.-H., Völkens, C. & Einarsson, P. 1995. Plate boundary deformation and continuing deflation of the Askja volcano, North Iceland, determined with GPA, 1987-1993, *Bull Volcanol.*, **57**(2), 136-145, doi:10.1007/BF00301404.
- Cattin, R., Doubre, C., de Chabaliere, J.-B., King, G., Vigny, C., Avouac, J.-P., & Ruegg, J.-C., 2005. Numerical modelling of quaternary deformation and post-rifting displacement in the Asal-Ghoubbet rift (Djibouti, Africa), *Earth Planet. Sci. Lett.*, **239**, 352-367, doi:10.1016/j.epsl.2005.07.028.
- Darbyshire, F.A., Priestley, K.F., White, R.S., Stefánsson, R., Gudmundsson, G.B. & Jakobsdóttir, S.S., 2000. Crustal structure of central and northern Iceland from analysis of teleseismic receiver functions, *Geophys. J. Int.*, **143**, 163-184.
- Decker, R.W., Einarsson, P., & Mohr, P.A., 1971. Rifting in Iceland: new geodetic data, *Science*, **173**, 530-533.
- Decker, R.W., Einarsson, P., & Plumb, R., 1976. Rifting in Iceland: measuring horizontal movements, *Soc. Sci. Isl. Greinar*, **5**, 61-71.
- DeMets, C., Gordon, R.G., Argus, D.F. & Stein, S., 1994. Effect of recent revisions to the geomagnetic reversal time scale on estimates of current plate motions, *Geophys. Res. Lett.*, **21**(20), 2191-2194.
- DeMets, C., Gordon, R. & Argus, D., 2010. Geologically current plate motions, *Geophys. Res. Int.*, **181**, 1-80, doi:10.1111/j.1365-246X.2009.04491.x.
- de Zeeuw-van Dalfsen, E., Pedersen, R., Hooper, A. & Sigmundsson, F., 2012. Subsidence of Askja caldera 200-2009: Modelling of deformation processes at an extensional plate boundary, constrained by time series InSAR analysis, *J. Volcanol. Geotherm. Res.*, **213-214**, 72-82, doi:10.1016/j.jvolgeores.2011.11.004.
- de Zeeuw-van Dalfsen, E., Pedersen, R., Sigmundsson, F. & Pagli, C., 2004. Satellite radar interferometry 1993-1999 suggests deep accumulation of magma near the crust-mantle boundary at the Krafla volcanic system, Iceland, *Geophys. Res. Lett.*, **31**(L13611), 1-5, doi:10.1029/2004GL020059.
- de Zeeuw-van Dalfsen, E., Rymer, H., Sturkell, E., Pedersen, R., Hooper, A., Sigmundsson, F. & Ófeigsson, B., 2013. Geodetic data shed light on ongoing caldera subsidence at Askja, Iceland, *Bull. Volcanol.*, **79**, 1-13, doi:10.1007/s00445-013-0709-2.
- Dick, H.B., Lin, J. & Schouten, H., 2003. An ultraslow-spreading class of ocean ridge, *Nature*, **426**, 405-412.
- Einarsson, P., 1991. Earthquakes and present-day tectonism in Iceland, *Tectonophysics*, **189**, 261-279.

- Einarsson, P., 2001. Structure and evolution of the Iceland hotspot, *Deutsche Geophysikalische Gesellschaft, Mitteilungen*, 1/2001, 11–14.
- Einarsson, P., 2008. Plate boundaries, rift and transforms in Iceland, *Jökull*, **58**, 35–58.
- Einarsson, P., Sigmundsson, F., Sturkell, E., Árnadóttir, Þ., Pedersen, R., Pagli, C. & Geirsson, H., 2006. Geodynamic signals detected by geodetic methods in Iceland. in *Festschrift for Prof. Seeber*, pp. 39–57, ed. Hirt, C., Wissenschaftliche Arbeiten der Fachrichtung Geodäsie und Geoinformatik der Universität Hannover, 258, Germany.
- Fleming, K., Martinec, Z., & Wolf, D., 2007. Glacial-isostatic adjustment and the viscosity structure underlying the Vatnajökull Ice Cap, Iceland, *Pure Appl. Geophys.*, **164**, 751–768, doi:10.1007/s00024-007-0187-6.
- Flóvenz, O. & Sæmundsson, K., 1993. Heat flow and geothermal processes in Iceland, *Tectonophysics*, **225**, 123–138.
- Foulger, G.R., 2006. Older crust underlies Iceland, *Geophys. J. Int.*, **165**, 672–676, doi: 10.1111/j.1365-246X.2006.02941.x.
- Freed, A.M., Herring, T. & Bürgmann, R., 2010. Steady-state laboratory flow laws alone fail to explain postseismic observations, *Earth and Planet. Sci. Lett.*, **300**, 1–10, doi:10.1016/j.epsl.2010.10.005.
- Geirsson, H., LaFemina, P., Árnadóttir, T., Sturkell, E., Sigmundsson, F., Travis, M., Schmidt, P., Lund, B., Hreinsdóttir, S. & Bennett, R., 2012. Volcano deformation at active plate boundaries: Deep magma accumulation at Hekla volcano and plate boundary deformation in south Iceland, *J. Geophys. Res.*, **117**(B11409), 1–18, doi:10.1029/2012JB009400.
- Gerke, K., 1974. Crustal movements in the Myvatn- and in the Thingvallavatn- area, both horizontal and vertical, in *Geodynamics of Iceland and the North Atlantic Area*, edited by L. Kristjánsson, pp. 263–275, Reidel, Dordrecht.
- Guðmundsson, A., 1986. Formation of crustal magma chamber in Iceland, *Geology*, **14**, 167–166.
- Guðmundsson, A., 1987a. Tectonics of the Thingvellir fissure swarm, SW Iceland, *J. Structural Geology*, **9**(1), 61–69.
- Guðmundsson, A., 1987b. Formation and mechanics of magma reservoirs in Iceland, *Geophys. J. R. Astron. Soc.*, **91**, 27–41.
- Heki, K., Foulger, G.R., Julian, B.R. & Jahn, C.-H., 1993. Plate dynamics near divergent boundaries: Geophysical implications of postdrifting crustal deformation in NE Iceland, *J. Geophys. Res.*, **98**(B8), 14279–14297.
- Hjartardóttir, Á.R., 2013. Fissure swarms of the Northern Volcanic Rift Zone, Iceland, *Ph.D. Thesis*, Faculty of Earth Sciences, University of Iceland, Reykjavik, Iceland.
- Hirth, G., Teyssier, C. & Dunlap, W.J., 2001. An evaluation of quartzite flow laws based on comparisons between experimentally and naturally deformed rocks, *Int. J. Earth Sci.*, **90**, 77–87.
- Hofton, M.A. & Foulger, G.R., 1996. Postdrifting anelastic deformation around the spreading plate boundary, north Iceland I. Modeling of the 1987–1992 deformation field using a viscoelastic Earth structure, *J. Geophys. Res.*, **101**(B11), 25403–25421.
- Jacoby, W.R., Hartmann, O., Wallner, H., Smilde, P.L., Bürger, S., Sjöberg, L.E., Erlingsson, S., Wolf, D., Klemann, V., & Sasgen, I., 2009. Temporal gravity variations near shrinking Vatnajökull ice cap, Iceland, *Pure Appl. Geophys.*, **166**, 1283–1302, doi:10.1007/s00024-009-0499-9.
- Jakobsdóttir, S.S., 2008. Seismicity in Iceland: 1994–2007, *Jökull*, **58**, 75–100.
- Jakobsson, S.P., 1979. Outline of the petrology of Iceland, *Jökull*, **29**, 57–73.
- Jóhannesson, H., & Sæmundsson, K., 1998. Geological Map of Iceland, 1:500 000: Bedrock Geology, Icelandic Institute of Natural History.
- Jones, S.M. & MacLennan, J., 2005. Crustal flow beneath Iceland, *J. Geophys. Res.*, **110**(B09410), 1–19, doi:10.1029/2004JB003592.
- Jónsson, S., Einarsson, P. & Sigmundsson, F., 1997. Extension across a divergent plate boundary, the Eastern Volcanic rift zone, south Iceland, 1967–1994, observed with GPS and electronic distance measurements, *J. Geophys. Res.*, **102**, 11913–11929.
- Kaban, M.K., Flóvenz, Ó. & Pálmason, G., 2002. Nature of the crust-mantle transition zone and the thermal state of the upper mantle beneath Iceland from gravity modelling, *Geophys. J. Int.*, **149**, 281–299,

- doi:10.1046/j.1365-246X.2002.01622.x.
- Karato, S., 1997. Phase transformations and rheological properties of mantle minerals, in *Earth's Deep Interior*, pp. 223–272, ed. Croosley, D., Gordon and Breach.
- Karato, S. & Wu, P., 1993. Rheology of the upper mantle: A synthesis, *Science*, **260**, 771–778.
- Key, J., White, R.S., Soosalu, H. & Jakobsdóttir, S.S., 2011. Multiple melt injection along a spreading segment at Askja, Iceland, *Geophys. Res. Lett.*, **38**(L05301), 1–5, doi:10.1029/2010GL046264.
- Korenaga, J. & Karato, S., 2008. A new analysis of experimental data on olivine rheology, *J. Geophys. Res.*, **113**(B02403), 1–23, doi:10.1029/2007JB005100.
- LaFemina, P.C., Dixon, T.H., Malservisi, R., Árnadóttir, T., Sturkell, E., Sigmundsson, F. & Einarsson, P., 2005. Geodetic GPS measurements in south Iceland: Strain accumulation and partitioning in a propagating ridge system, *J. Geophys. Res.*, **110**(B11405), 1–21, doi:10.1029/2005JB003675.
- MacLennan, J., McKenzie, D. & Gronvöld, K., 2001. Plume-driven upwelling under central Iceland, *Earth and Planet. Sci. Lett.*, **194**, 67–82.
- Moore, J.G., Jakobsson, S.P., & Hólmjárn, J., 1992. Subsidence of Surtsey volcano, *Bull. Volcanol.*, **55**, 17–24.
- Morishima, H., Kato, T., Suto, M., Ohtani, E., Urakawa, S., Utsumi, W., Shimomura, O. & Kikegawa, T., 1994. The phase boundary between alpha- and beta- Mg₂SiO₄ determined by in situ X-ray observation, *Science*, **265**, 1202–1203.
- Niemczyk, V.O. & Emschermann, E., 1943. Sonderdreiecksmessung auf Island zur Feststellung feinsten Erdkrustenbewegungen, in *Spalten auf Island*, pp. 80–113, ed. Niemczyk, O., Verlag Von Konrad Wittwer, Stuttgart, Germany.
- Okada, Y., 1985. Surface deformation due to shear and tensile faults in a half-space, *Bull. Seis. Soc. Ame.*, **75**(4), 1135–1154.
- Pagli, C., Sigmundsson, F., Árnadóttir, T., Einarsson, P. & Sturkell, E., 2006. Deflation of the Askja volcanic system: Constraints on the deformation source from combined inversion of satellite radar interferograms and GPS measurements, *J. Volcanol. Geotherm. Res.*, **152**(1), 97–108, doi:10.1016/j.jvolgeores.2005.09.014.
- Pagli, C., Sigmundsson, F., Lund, B., Sturkell, E., Geirsson, H., Einarsson, P., Árnadóttir, T. & Hreinsdóttir, S., 2007. Glacio-isostatic deformation around the Vatnajökull ice cap, Iceland, induced by recent climate warming: GPS observations and finite element modelling, *J. Geophys. Res.* **112**(B08405), 1–12, doi:10.1029/2006JB004421.
- Pagli, C., Wang, H., Wright, T.J., Calais, E. & Lewi, E., 2014. Current plate boundary deformation of the Afar rift from a 3-D velocity field inversion of InSAR and GPS, *J. Geophys. Res. Solid Earth*, **119**, 1–14, doi:10.1002/2014JB011391.
- Pedersen, R., Sigmundsson, F. & Masterlark, T., 2009. Rheologic controls on inter-rifting deformation of the Northern Volcanic Zone, Iceland, *Earth Planet. Sci. Lett.*, **281**, 14–26, doi:10.1016/j.epsl.2009.02.003.
- Pollitz, F.F. & Sacks, I.S., 1996. Viscosity structure beneath northeast Iceland, *J. Geophys. Res.*, **101**(B8), 17,771–17,793, doi: 10.1029/96JB01074.
- Ruedas, T., Schmeling, H., Marquart, G., Kreutzmann, A. & Junge, A., 2004. Temperature and melting of a ridge-centered plume with application to Iceland, Part I. Dynamics and crust production, *Geophys. J. Int.*, **158**, 729–743, doi:10.1111/j.1365-246X.2004.02311.x.
- Sæmundsson, K., 1974. Evolution of the axial rift zone in northern Iceland and the Tjornes Fracture Zone, *Geol. Soc. Ame. Bull.*, **85**, 495– 504.
- Sæmundsson, K., 1992. Geology of the Thingvallavatn area, *Oikos*, **64**, 40– 68.
- Saria, E., Calais, E., Stamps, D.S., Delvaux, D. & Hartnady, C.J.H., 2014. Present-day kinematics of the East African Rift, *J. Geophys. Res. Solid Earth*, **119**, 3584–3600, doi:10.1002/2013JB010901.
- Savage, J.C. & Burford, R.O., 1973. Geodetic determination of relative plate motion in central California, *J. Geophys. Res.*, **78**, 832–854.
- Scheiber-Enslin, S.E., LaFemina, P.C., Sturkell, E., Hooper, A.J. & Webb, S.J., 2011. Geodetic Investigation of plate spreading along a propagating ridge: the Eastern Volcanic Zone, Iceland, *Geophys. J. Int.*, 1–20, doi:10.1111/j.1365-246X.2011.05243.x.
- Schmeling, H. & Marquart, G., 2008. Crustal accretion and dynamic feedback on mantle melting of a ridge centred plume: the Iceland case, *Tectonophys.*, **447**, 31–52.

- Sella, G., Dixon, T.H., & Mao, A.L., 2002. REVEL: A model for recent plate velocities from space geodesy, *J. Geophys. Res. Solid Earth*, **107**(4), 1-31, doi:10.1029/2000JB000033.
- Sigmundsson, F., 2006. *Iceland Geodynamics: Crustal Deformation and Divergent Plate Tectonics*, Praxis Publishing.
- Sigmundsson, F. & Einarsson, P., 1992. Glacio-isostatic crustal movements caused by historical volume change of the Vatnajökull ice cap, Iceland, *Geophys. Res. Lett.*, **19**(21), 2123-2126.
- Sigmundsson, F., Einarsson, P., Bilham, R. & Sturkell, E., 1995. Rift transform kinematics in South Iceland; deformation from Global Positioning System measurements, 1986 to 1992, *J. Geophys. Res.*, **100** (B4), 6235-6248, doi:10.1029/95JB00155.
- Sigmundsson, F., Hooper, A., Hreinsdóttir, S., Vogfjörð, K.S., Ófeigsson, B.G., Heimisson, E.R., Dumont, S., Parks, M., Spaans, K., Gudmundsson, G.B., Drouin, V., Arnadóttir, T., Jónsdóttir, K., Gudmundsson, M.T., Högnadóttir, T., Fridriksdóttir, H.M., Hensch, M., Einarsson, P., Magnússon, E., Samsonov, S., Brandsdóttir, B., White, R.S., Ágústsdóttir, T., Greenfield, T., Green, R.G., Hjartardóttir, A.R., Pedersen, R., Bennett, R.A., Geirsson, H., La Femina, P.C., Björnsson, H., Pálsson, F., Sturkell, E., Bean, C.J., Möllhoff, M., Braiden, A.K. & Eibl, E.P.S., 2015. Segmented lateral dyke growth in a rifting event at Bárðarbunga volcanic system, Iceland, *Nature*, **517**, 191–195, doi:10.1038/nature14111.
- Sigurdsson, H. & Sparks, S., 1978. Rifting episode in North Iceland in 1874-1875 and the eruptions of Askja and Sveinagja, *Bull. Volcanol.*, **41**, 149-167.
- Sinton, J., Grönvold, K., & Sæmundsson, K., 2005. Postglacial eruptive history of the Western Volcanic Zone, Iceland, *Geochem. Geophys. Geosys. G³*, **6**(12), 1-34, doi:10.1029/2005GC001021.
- Soosalu, H., Key, J., White, R.S., Knox, C., Einarsson, P. & Jakobsdóttir, S.S., 2010. Lower-crustal earthquakes caused by magma movement beneath Askja volcano on the north Iceland rift, *Bull. Volcanol.*, **72**, 55-62, doi:10.1007/s00445-009-0297-3.
- Sjöberg, L.E., Pan, M., Erlingsson, S., Asenjo, E. & Arnason, K., 2004. Land uplift near Vatnajökull, Iceland, as observed by GPS in 1992, 1996 and 1999, *Geophys. J. Int.*, **159**, 943-948, doi:10.1111/j.1365-246X.2004.02353.x.
- Stefánsson, R., Böðvarsson, R., Slunga, R., Einarsson, P., Jakobsdóttir, S.S., Bungum, H., Gregersen, S., Havskov, J., Hjelme, J. & Korhonen H., 1993. Earthquake prediction research in the south Iceland seismic zone and the SIL project, *Bull. Seism. Soc. Am.*, **83**(3), 696-716.
- Sturkell, E., Einarsson, P., Geirsson, H., Tryggvason, E., Moore, J.G., & Ólafsdóttir, R., 2009. Precision levelling and geodetic GPS observations performed on Surtsey between 1967 and 2002, *Surtsey Res.*, **12**, 39-47.
- Sturkell, E. & Sigmundsson, F., 2000. Continuous deflation of the Askja caldera, Iceland, during the 1983-1998 noneruptive period, *J. Geophys. Res.* **105**(B11), 25671-25684, doi:10.1029/2000JB900178.
- Sturkell, E., Sigmundsson, F. & Slunga, R., 2006a. 1983–2003 decaying rate of deflation at Askja caldera: Pressure decrease in an extensive magma plumbing system at a spreading plate boundary, *Bull. Volcanol.*, **68**, 727–735, doi:10.1007/s00445-005-0046-1.
- Sturkell, E., Einarsson, P., Sigmundsson, F., Geirsson, H., Ólafsson, H., Pedersen, P., de Zeeuw-van Dalftsen, E., Linde, A.T., Sacks, S.I. & Stefánsson, R., 2006b. Volcano geodesy and magma dynamics in Iceland, *J. Volcanol. Geotherm. Res.*, **150**, 14–34, doi:10.1016/j.jvolgeores.2005.07.010.
- Toomey, D.R., 2012. Piecing together rifts, *Nature Geoscience*, **5**, 235236.
- Tryggvason, E., 1974. Vertical crustal movement in Iceland, in *Geodynamic of Iceland and the North Atlantic Area*, edited by L. Kristjánsson, pp. 241-262, Reidel, Dordrecht.
- Tryggvason, E., 1980. Subsidence events in the Krafla area, north Iceland, 1975-1979, *J. Geophys.*, **47**, 141-153.
- Tryggvason, E., 1982. Recent ground deformation in continental and oceanic rift zones, in Palmason, G. (ed.), *Continental and Oceanic Rifts (17-29)*, *Geodynamic Series 8*, AGU, Washington.
- Tryggvason, E., 1990. Höggun Almanagjár. Mælingar á Þingvöllum 1990 (Displacement of Almanagja. Measurements at Thingvellir 1990), Nord. Volcanol. Inst., Univ. of Iceland, Reykjavik.
- Turcotte, D.L. & Schubert, G., 2002. *Geodynamics*, 2nd edn, Cambridge University Press.
- Vigny, C., de Chabaliér, J.-B., Ruegg, J.-C., Huchon, P., Feigl, K.L., Cattin, R., Asfaw, L. & Kanbari, K., 2007. Twenty-five years of geodetic measurements along the Tadjoura-Asal rift system, Djibouti, East Africa, *J. Geophys. Res.*, **112**(B06410), 1-12, doi:10.1029/2004JB003230.

- White, R.S., Drew, J., Martens, H.K., Key, A.J., Soosalu, H. & Jakobsdóttir, S.S., 2011. Dynamic of dyke intrusion in the mid-crust of Iceland, *Earth and Planet. Sci. Lett.*, **304**, 300-312, doi:10.1016/j.epsl.2011.02.038.
- Wolf, D., Barthelmes, F. & Sigmundsson, F., 1997. Predictions of deformation and gravity change caused by recent melting of the Vatnajökull ice cap, Iceland, pp. 311-319, Springer-Verlag, Berlin.
- Wright, T.J., Ebinger, J., Ayele, A., Yirgu, G., Keir, D. & Stork, A., 2006. Magma-maintained rift segmentation at continental rapture in the 2005 Afar dyking episode, *Nature*, **442**(7100), 291-294.
- Wright, T.J., Sigmundsson, F., Pagli, C., Belachew, M., Hamling, I.J., Brandsdóttir, B., Keir, D., Ayele, A., Ebinger, C., Einarsson, P., Lewi, E. & Calais, E., 2012. Geophysical constraints on the dynamics of spreading centres from rifting episodes on land, *Nature Geoscience*, **5**, 242-250, doi:10.1038/NGEO1428.